Sciencexpress Reports

Speleothems Reveal 500,000-Year History of Siberian Permafrost

A. Vaks,[1]* O. S. Gutareva,[2] S. F. M. Breitenbach,[3] E. Avirmed,[4] A. J. Mason,[1] A. L. Thomas,[1] A. V. Osinzev,[5] A. M. Kononov,[2] G. M. Henderson[1]

[1]Department of Earth Sciences, University of Oxford, Oxford OX1 3AN, UK. [2]Institute of Earth's Crust, Russian Academy of Sciences, Siberian Branch, 128 Lermontova Street, Irkutsk 664033, Russia. [3]Swiss Federal Institute of Technology Zürich (ETHZ), CH-8092 Zurich, Switzerland. [4] Institute of Geography, Mongolian Academy of Sciences, 210620 UlaanBaatar, Mongolia. [5]Arabica Speleological Club, Mamin-Sibiryak Street, Box 350, Irkutsk 554082, Russia.

*To whom correspondence should be addressed. E-mail: anton.vaks@earth.ox.ac.uk

Soils in permafrost regions contain twice as much carbon as the atmosphere, and permafrost has an important influence of the natural and built environment at high northern latitudes. The response of permafrost to warming climate is uncertain and occurs on timescales longer than has been assessed by direct observation. In this study, we date periods of speleothem growth in a north-south transect of caves in Siberia to reconstruct the history of permafrost in past climate states. Speleothem growth is restricted to full interglacial conditions in all studied caves. In the northernmost cave (at 60°N), no growth has occurred since Marine Isotopic Stage (MIS) 11. Growth at that time indicates that global climates only slightly warmer than today are sufficient to thaw significant regions of permafrost.

Permafrost regions (in which the ground is frozen throughout the year) cover 24% of the northern-hemisphere land surface and hold ~1700 Gt of organic carbon. When it thaws it releases CO_2 and CH_4, turning a long-term carbon sink into a source and enhancing the greenhouse effect (*1*, *2*). Permafrost degradation also intensifies thermo-karst development, coastline erosion and liquefaction of ground previously cemented by ice. The latter endangers infrastructure including major Siberian oil and gas facilities (*3*). An ability to predict the extent of future permafrost degradation is desirable.

Assessing the response of permafrost to changing climate is challenging. Significant warming and thawing of local permafrost conditions are seen in instrumental records during the last 20 years (*4*) but permafrost response at regional scale is slow to respond to warming and instrumental records are insufficient to capture the long-term behavior. To understand the long-term response of permafrost to climate change requires knowledge of past permafrost conditions. Dating of organic material (*4*) or ground ice (*5*) can indicate the age of existing permafrost, but cannot reveal the longer-term history of permafrost.

In this study, we use cave carbonates (speleothems) as a tool to date past permafrost and its relationship to global climate. Vadose speleothems (stalactites, stalagmites and flowstones) form when meteoric waters (i.e., water originating from atmospheric precipitation) seep through the vadose zone into caves. Cave temperatures usually approximate the local mean annual air temperatures (MAAT), because of buffering by the surrounding rock (*6*). When cave temperatures drop below 0°C, waters freeze and speleothem growth ceases. Speleothems found in modern permafrost regions are therefore relicts from warmer periods before permafrost formed (*7–9*). Absence of water also prevents speleothem growth in arid settings, so speleothem growth episodes in modern deserts are proxies for past wet periods (*10*). Because speleothems can be robustly and precisely dated with U-Th techniques, they provide a detailed history of periods when liquid water was available, and both permafrost and desert conditions were absent.

We reconstruct the history of Siberian permafrost (and the aridity of the Gobi Desert) during the last ~500 kyr using U-Th dating of speleothems in six caves along a north-south transect in northern Asia from Eastern Siberia at 60.2°N to the Gobi Desert at 42.5°N (Fig. 1). The northernmost cave - Lenskaya Ledyanaya sits today on the boundary of continuous permafrost with MAAT substantially below 0°C (*11*). The permafrost type changes to the south-west to discontinuous, sporadic, and then to permafrost-free conditions (*12*) (Fig. 1). Annual precipitation in this Siberian region is 400-600 mm/y falling mainly during summer. To the south, in the Gobi, MAAT ranges from +2°C to +8°C and little precipitation falls (200-80 mm/y) (*13*).

Speleothem thickness provides an indication of long-term liquid-water availability along the transect. Only 8 cm of growth is seen in the northernmost cave, increasing to ~70 cm in the caves of southern Siberia and decreasing again to less than 30 cm in the Gobi. As expected, southern Siberia is more suitable for speleothem growth than the cold north or the dry south. All recovered speleothems show a texture of calcium-carbonate layers alternating with growth hiatuses (see supplementary materials).

Thirty-six speleothems were collected from the caves and 111 U-Th ages conducted (Fig. 2A). In each speleothem, at least one sample was taken from the outermost layer and from each section of growth (i.e., between hiatuses) inward, until the limits of the U-Th chronology were reached (~500 ka) to assess all periods of growth. A full description of the samples, and their sub-sampling and dating is given in the supplementary materials.

The youngest speleothem growth in the region of modern continuous permafrost (i.e., at 60°N) occurred during interglacial MIS-11, contrasting with the center of the transect where speleothems grew during all interglacials (Fig. 2, A and B). Age ranges in southern Siberia also demonstrate that the duration of speleothem deposition in MIS-11 was longer than during subsequent interglacials. These observations indicate that permafrost thawing during MIS-11 was more extensive than at any other point during the last 450 kyr and extended northward of 60°N, significantly further north than the present limit of continuous permafrost. Some similar thawing may also have occurred at MIS-13 in this most northerly cave. The absence of any observed speleothem growth since MIS 11 in the northerly Lenskaya Ledyanaya cave (despite dating outer edges of 7 speleothems), suggests the permanent presence of permafrost at this latitude since the end of MIS-11. Speleothem growth in this cave occurred in early MIS-11, ruling out the possibility that the unusual length of MIS-11 caused the permafrost thawing.

MIS-11 was also characterized by wetter conditions in the Mongolian Gobi Desert, as shown by two ages from Shar-Khana Cave speleothems (Fig. 2A), which contrast with the absence of growth during subsequent interglacials. The existence of a humid event in the Gobi during early MIS-11 is supported by mollusk assemblages from Chinese Loess Plateau (*14*), and by the dominance of input into Lake Baikal via the Selenga River during MIS-11 (*15*).

The degradation of permafrost at 60°N during MIS-11 allows an assessment of the warming required globally to cause such extensive change in the permafrost boundary. There is significant evidence that

MIS-11 was the warmest of recent interglacials, including the presence of boreal forest on South Greenland at that time (*16*), the absence of ice-rafted debris in the North Atlantic (*17*), increased sea levels (*18*), and higher sea-surface temperatures (SST) in the tropical Pacific (*19*–*21*). Mg/Ca reconstructions (*20*, *21*) indicate that SST of the Pacific Warm Pool (PWP) reached >30°C in early MIS-11, compared to 29.5°C in MIS-5.5 and ~28.5°C during the pre-industrial Late Holocene (Fig. 2D). This tropical heat was transported poleward (*22*) and there is evidence of unusual warmth in Siberia during MIS-11, evidenced by the high fraction of biogenic silica in the sediments of Lake Baikal (*23*) (Fig. 2C) and high spruce pollen content in Lake El'gygytgyn, suggesting local temperatures 4-5°C above present (*24*). When PWP temperatures reach 30°C this appears to cause more pronounced warming of northern continents, and lead to significant northward migration of the permafrost boundary.

Periods of Siberian speleothem growth since MIS-11 suggest a close link between greenhouse warming/global temperatures and permafrost extent. After a brief post MIS-11 hiatus in growth (from 370 to 355 ka), coinciding with a minimum in atmospheric CO_2 and in PWP SST during MIS-10 (Fig. 2, D and F), significant thicknesses of speleothem grew in Southern Siberia during MIS-9 as greenhouse gases returned to higher values. Speleothems also grew actively during MIS-5.5 and the Holocene (>5 cm) when CO_2 levels were high. In contrast, growth during MIS-7, a period of lower CO_2 and cooler global conditions, is minimal (maximum 1.5 cm in any studied cave) and no growth is observed during MIS-5.4 to 5.1. Conditions during MIS-7 were at the very limit for growth in southern Siberia: speleothems grew during MIS-7.3 and 7.1 in Okhotnichya Cave (52°N) but only during MIS-7.1 just to the north at Botovskaya Cave (55°N). No growth occurred during MIS-7.5 at either cave despite higher concentrations of CO_2 and CH_4 than later in MIS-7 (*25*, *26*) and high PWP SST (Fig. 2, D to F) (*20*, *21*). Lake Baikal biogenic silica (*23*) and the percentage of arboreal pollen in Lake El'gygytgyn sediments (*27*) are also lower during MIS-7.5 than during MIS-7.3 and 7.1. Lower local summer insolation during MIS-7.5 (Fig. 2G) (*28*) suggests a role for local insolation in overprinting a Siberian climate dominantly controlled by global greenhouse gas levels.

U-Th dating of Siberian speleothem growth during recent interglacials allows detailed comparison of permafrost history with other aspects of the global climate system (Fig. 3). During MIS-5.5, speleothems started growing between 128.7 and 127.3 ka, and ended between 119.2 and 118.1 ka (determined from Bayesian analysis of U-Th data using OxCal-4.1; see supplementary materials). The permafrost thawing initiated when insolation was close to its maximum and greenhouse gases had just reached maximum values. Holocene permafrost degradation at our sites lags maximum insolation and greenhouse gas concentrations slightly, and starts between 10.0 and 9.8 ka. This lag may be due to the time required for permafrost to thaw at the slightly lower insolation and CO_2 levels of the Holocene (relative to MIS-5.5).

Overall, dated periods of speleothem growth allow an assessment of the relationship between global temperature and permafrost extent. PWP SST was 0.5-1.0°C higher during MIS-5.5 and ~1.5°C higher during early MIS-11 relative to the pre-industrial Late Holocene (Fig. 2D) (*20*, *21*). Using PWP SST as a surrogate for global temperature (*20*) suggests that increase in global temperatures by 0.5-1.0°C will degrade only non-continuous permafrost in southern Siberia with the Gobi Desert remaining arid. Warming of ~1.5°C (i.e., as in MIS-11) may cause a substantial thaw of continuous permafrost as far north as 60°N, and create wetter conditions in the Gobi Desert. Such warming is therefore expected to dramatically change the environment of continental Asia, and can potentially lead to substantial release of carbon trapped in the permafrost into the atmosphere.

References and Notes

1. G. Grosse *et al*., Vulnerability and feedbacks of permafrost to climate change. *EOS* **92**, 73 (2011). doi:10.1029/2011EO090001
2. E. A. G. Schuur *et al*., Vulnerability of permafrost carbon to climate change: Implications for the global carbon cycle. *Bioscience* **58**, 701 (2008). doi:10.1641/B580807
3. O. Anisimov, S. Reneva, Permafrost and changing climate: the Russian perspective. *AMBIO* **35**, 169 (2006).
4. Y. K. Vasil'chuk, J.-C. Kim, A. C. Vasil'chuk, AMS14C dating and stable isotope plots of Late Pleistocene ice-wedge ice. *Nucl. Instrum. Methods Phys. Res. B* **223–224**, 650 (2004). doi:10.1016/j.nimb.2004.04.120
5. D. A. Gilichinsky *et al*., Dating of syngenetic ice wedges in permafrost with ^{36}Cl. *Quat. Sci. Rev.* **26**, 1547 (2007). doi:10.1016/j.quascirev.2007.04.004
6. H. P. Schwarcz, in *Handbook of Environmental Isotope Geochemistry*, P. Fritz, J. C. Fontes, Eds. (Elsevier, Amsterdam, 1986), vol. 2, pp. 271–300.
7. R. A. Cliff, C. Spötl, A. Mangini, U-Pb dating of speleothems from Spannagel Cave, Austrian Alps: A high resolution comparison with U-series ages. *Quat. Geochronol.* **5**, 452 (2010). doi:10.1016/j.quageo.2009.12.002
8. B. Lauriol, D. C. Ford, J. Cinq-Mars, W. A. Morris, The chronology of speleothem deposition in northern Yukon and its relationships to permafrost. *Can. J. Earth Sci.* **34**, 902 (1997). doi:10.1139/e17-075
9. S. E. Lauritzen, High-resolution paleotemperature proxy record for the last interglaciation based on Norwegian speleothems. *Quat. Res.* **43**, 133 (1995). doi:10.1006/qres.1995.1015
10. A. Vaks, M. Bar-Matthews, A. Matthews, A. Ayalon, A. Frumkin, Middle-Late Quaternary paleoclimate of northern margins of the Saharan-Arabian Desert: Reconstruction from speleothems of Negev Desert, Israel. *Quat. Sci. Rev.* **29**, 2647 (2010). doi:10.1016/j.quascirev.2010.06.014
11. Philip's Modern School Atlas, 95th Edition (Philip's/Octopus, London, 2007).
12. A. Jones *et al*., Eds., *Soil Atlas of the Northern Circumpolar Region* (Publication Office of the European Union, Luxembourg, 2010).
13. D. Dorjotov, N. Orshikh, T. Oyunchimeg, *Geographic Atlas of Mongolian Republic* (Mongolian Institute of Geodesy and Cartography, Ulaanbaatar, 2004). [in Mongolian]
14. N. Wu *et al*., Climatic conditions recorded by terrestrial mollusc assemblages in the Chinese Loess Plateau during marine Oxygen Isotope Stages 12–10. *Quat. Sci. Rev.* **26**, 1884 (2007). doi:10.1016/j.quascirev.2007.04.006
15. A. W. Mackay *et al*., Reconstructing hydrological variability in Lake Baikal during MIS 11: An application of oxygen isotope analysis of diatom silica. *J. Quaternary Sci.* **23**, 365 (2008). doi:10.1002/jqs.1174
16. A. de Vernal, C. Hillaire-Marcel, Natural variability of Greenland climate, vegetation, and ice volume during the past million years. *Science* **320**, 1622 (2008). doi:10.1126/science.1153929 Medline
17. J. F. McManus, D. W. Oppo, J. L. Cullen, A 0.5-million-year record of millennial-scale climate variability in the north atlantic. *Science* **283**, 971 (1999). doi:10.1126/science.283.5404.971 Medline
18. M. E. Raymo, J. X. Mitrovica, Collapse of polar ice sheets during the stage 11 interglacial. *Nature* **483**, 453 (2012). doi:10.1038/nature10891 Medline
19. L. Ortlieb, A. Diaz, N. Guzman, A warm interglacial episode during oxygen isotope stage 11 in northern Chile. *Quat. Sci. Rev.* **15**, 857 (1996). doi:10.1016/S0277-3791(96)00062-5
20. J. Hansen *et al*., Global temperature change. *Proc. Natl. Acad. Sci. U.S.A.* **103**, 14288 (2006). doi:10.1073/pnas.0606291103 Medline
21. M. Medina-Elizalde, D. W. Lea, The mid-Pleistocene transition in the tropical Pacific. *Science* **310**, 1009 (2005). doi:10.1126/science.1115933 Medline
22. A. J. Dickson *et al*., Oceanic forcing of the Marine Isotope Stage 11 interglacial. *Nat. Geosci.* **2**, 428 (2009). doi:10.1038/ngeo527
23. A. A. Prokopenko *et al*., Biogenic silica record of the Lake Baikal response to climatic forcing during the Brunhes. *Quat. Res.* **55**, 123 (2001). doi:10.1006/qres.2000.2212
24. M. Melles *et al*., 2.8 million years of Arctic climate change from Lake El'gygytgyn, NE Russia. *Science* **337**, 315 (2012). doi:10.1126/science.1222135 Medline
25. L. Loulergue *et al*., Orbital and millennial-scale features of atmospheric CH_4 over the past 800,000 years. *Nature* **453**, 383 (2008). doi:10.1038/nature06950 Medline
26. D. Lüthi *et al*., High-resolution carbon dioxide concentration record 650,000-800,000 years before present. *Nature* **453**, 379 (2008). doi:10.1038/nature06949 Medline

27. N. R. Nowaczyk *et al*., Magnetostratigraphic results from impact crater Lake El'gygytgyn, northeastern Siberia: A 300 kyr long high-resolution terrestrial palaeoclimatic record from the Arctic. *Geophys. J. Int.* **150**, 109 (2002). doi:10.1046/j.1365-246X.2002.01625.x
28. J. Laskar *et al*., A long-term numerical solution for the insolation quantities of the Earth. *Astron. Astrophys.* **428**, 261 (2004). doi:10.1051/0004-6361:20041335
29. J. Brown, J. O. J. Ferrians, J. A. Heginbottom, E. S. Melnikov, National Snow and Ice Data Center/World Data Center for Glaciology, Boulder, CO, 2001.
30. L. E. Lisiecki, M. E. Raymo, A Pliocene-Pleistocene stack of 57 globally distributed benthic $\delta^{18}O$ records. *Paleoceanography* **20**, PA1003 (2005). doi:10.1029/2004PA001071
31. Y. Wang *et al*., Millennial- and orbital-scale changes in the East Asian monsoon over the past 224,000 years. *Nature* **451**, 1090 (2008). doi:10.1038/nature06692 Medline
32. S. O. Rasmussen *et al*., A new Greenland ice core chronology for the last glacial termination. *J. Geophys. Res.* **111**, D06102 (2006). doi:10.1029/2005JD006079
33. See references 16 to 19 in the supplementary materials.

Acknowledgments: This article is dedicated to the memory of Prof. Y. Trzhcinski, who during the last months of his life made a big effort to establish the cooperation between University of Oxford and Institute of Earth's Crust (IEC) in Irkutsk. Thanks to D. Sokolnikov and other 'Arabica' members, E. Kozireva (IEC), V. Alexioglo and V. Balaev from Lensk for their help during the fieldwork in Siberia, Mongolian Speleological Society for their help with the fieldwork in Mongolia; to J. Fritz and L. Zehnder (ETH Zurich) for drawing Fig. 1 and for assistance with XRD analyses respectively; to C. Day, V. Ersek, P. Holdship, O. Green, S. Wyatt, Y. Nakajima, P. Pousada Solino and others from University of Oxford for the help with the laboratory work, administration issues and fruitful discussions. This work was funded by NERC Fellowship NE/G013829/1, Royal Society grant JP080831 and Russian Foundation for Basic Research joint grant 09-05-92605 KO_a.

Supplementary Materials
www.sciencemag.org/cgi/content/full/science.1228729/DC1
Materials and Methods
Supplementary Text
Figs. S1 to S16
Tables S1 to S3
References

13 August 2012; accepted 6 February 2013

Published online 21 February 2013
10.1126/science.1228729

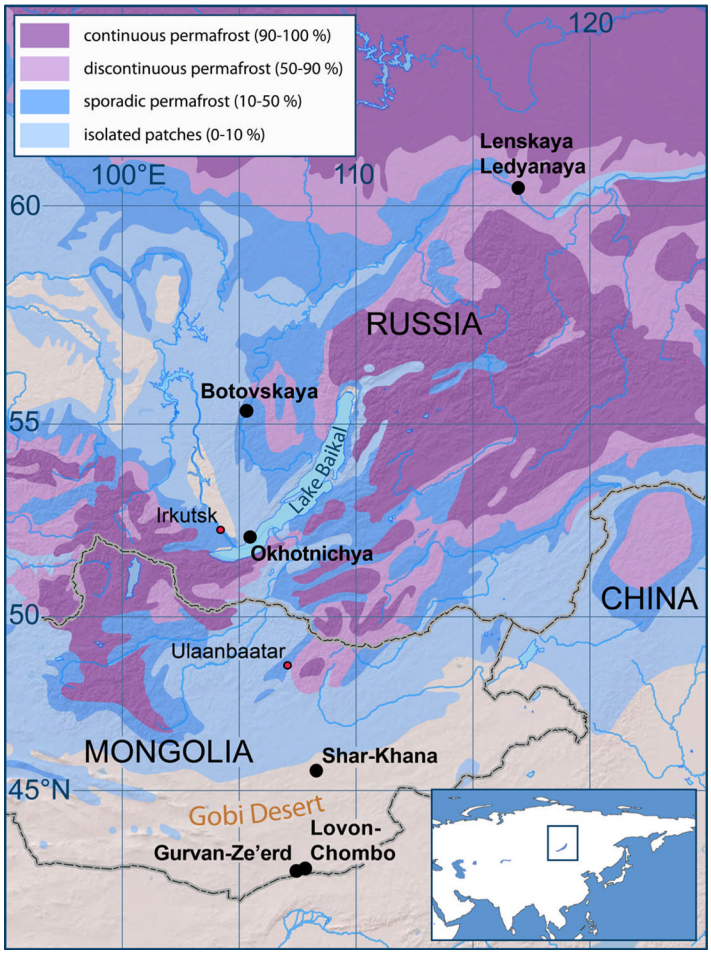

Fig. 1. Map showing the extent of permafrost types in eastern Siberia, the Gobi Desert, and the location of studied caves (black circles). Permafrost data are taken from Brown *et al*. (2001) (*29*).

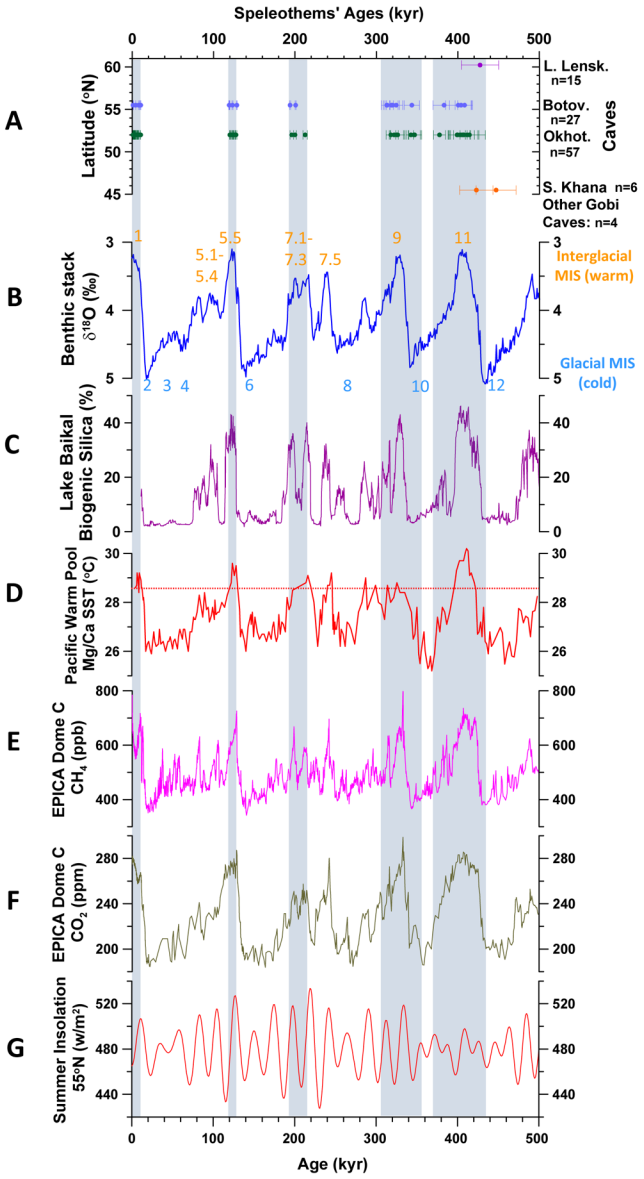

Fig. 2. (**A**) Distribution of speleothem U-Th ages (±2σ) in time and space (*n* – total number of U-Th age determinations per cave, including those beyond the U-Th range) with grey bars signifying periods of growth in Okhotnichya and Botovskaya caves. (**B**) Benthic $\delta^{18}O$ stack (*30*) with MIS numbers. (**C**) Concentration of biogenic silica in Lake Baikal sediments (%) (*23*). (**D**) Pacific Warm Pool Mg/Ca SST, with the pre-industrial Late Holocene SST shown by red horizontal fragmented line (*20*, *21*). (**E** and **F**) CH_4 and CO_2 records of EPICA Dome C respectively (*25*, *26*). (**G**) Summer insolation at 55°N (*28*). Speleothems with ages exceeding 500 ka (within ±2σ range) are not shown, but accounted for in *n*. Two samples SLL9-2-A+B and SOP-32-B are not included because they reflect a mixture of material from different layers; please refer to table S1.

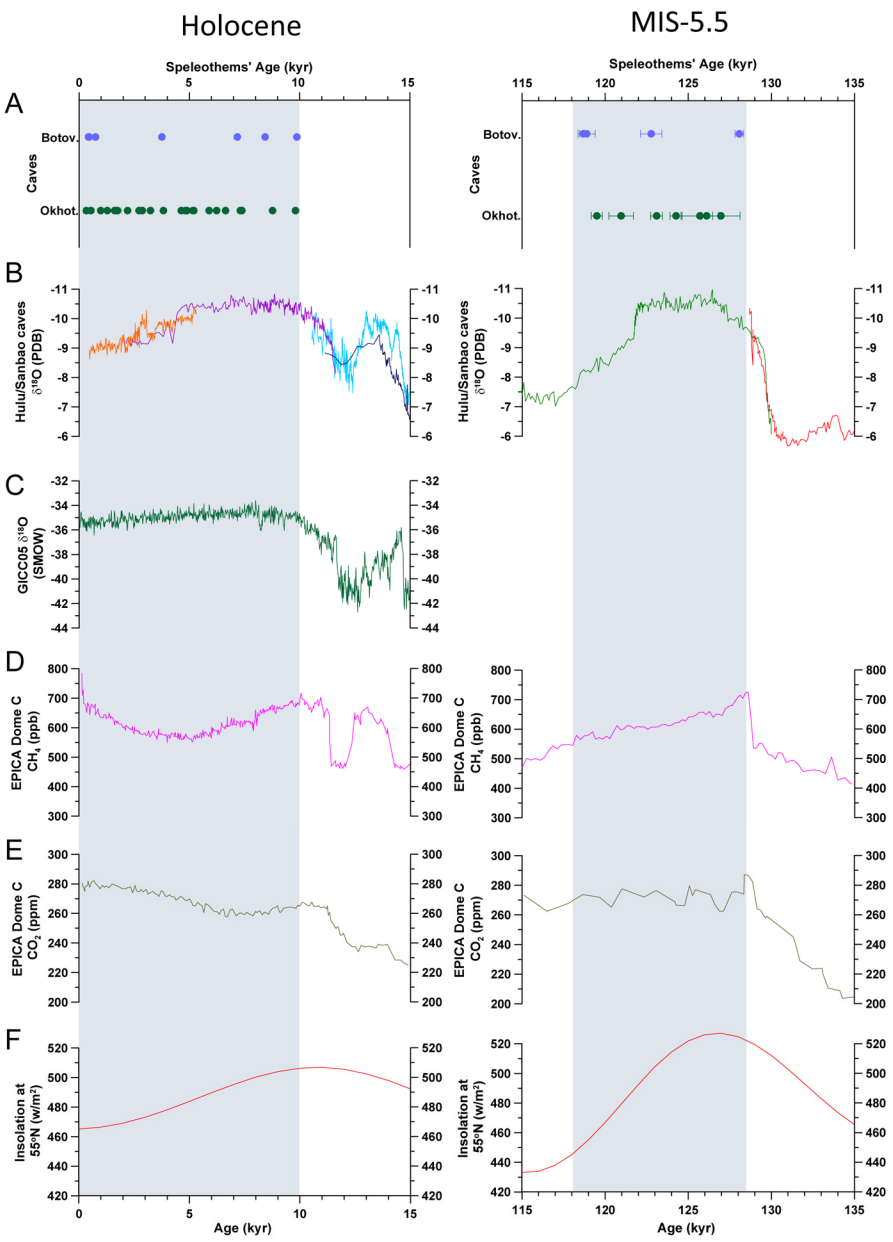

Fig. 3. Siberian speleothem growth periods during Holocene and MIS-5.5 (**A**) with grey bars indicating periods of growth. Compared with East-Asian Monsoon record from Hulu and Sanbao caves (**B**) (*31*), GICC05 $\delta^{18}O$ (**C**) (*32*, *33*), CH_4 (**D**) and CO_2 (**E**) records of EPICA Dome C (*25*, *26*), and 55°N summer insolation (**F**) (*28*).